Spatio-temporal distribution of dust storms – a global coverage using NASA TOMS aerosol measurements

György VARGA[1]

Abstract

Wind-blown dust and dust storms play important role in several environmental processes of our planet. Geographical distributions and seasonality patterns of major dust source areas were analysed in this paper by using the daily aerosol measurements of NASA's Total Ozone Mapping Spectrometer (TOMS) between 1979 and 2011. Spatial investigations of aerosol maps have confirmed that major source areas can be connected to specific geomorphological environments of distinct arid-semiarid regions with recent pluvial history. Largest dust activity can be observed in the topographical lows of Saharan and Arabian deserts, and in the intermountain, endorheic basins of Central Asia fed by fine-grained material from the adjacent mountain belts. Dust emissions are associated to regional seasonal, meteorological conditions; with typically high dust activity in spring and summer.

Keywords: dust storms, atmospheric dust, satellite measurements, geomorphological environments, meteorology

Introduction

Dust storms and deflated fine-grained aeolian mineral particles (<62.5 μm) are subjects of growing interest due to their multiple influences on climatic and other environmental processes (Harrison, S.P. *et al.* 2001; Kohfeld, K.E. and Tegen, I. 2007; Maher, B.A. *et al.* 2010; Pósfai, M. and Buseck, P.R. 2010; Shao, Y. *et al.* 2011). Wind-blown dust absorbs, scatters and reflects both the incoming shortwave solar and the outgoing longwave radiation, so modifies the energy-balance of our planet. Mineral particles can change the albedo of surface (Arimoto, R. 2001), cloud-formation processes (Rosenfeld, D. *et al.* 2001; Sassen, K. *et al.* 2003), chemical properties of precipitation (Roda, F. *et al.* 1993; Rogora, M. *et al.* 2004) and also have an effect on biogeochemical cycles through Fe fertilization of iron-limited oceanic ecosystems (Ridgewell, A.J. 2002). The far-travelled dust material incorporates

[1] Geographical Institute, Research Centre for Astronomy and Earth Sciences HAS, H-1112 Budapest, Budaörsi út 45. E-mail: varga.gyorgy@csfk.mta.hu

Table 1. Major environmental and climatic factors affecting the formation, size and frequency of dust storms

	Climate and meteorology	Geology and pedology	Geomorphology	Other factors
Formation of dust material	– aridity – temperature (values, distribution and freeze-thaw actions) – precipitation (amount, distribution and intensity) – evapotranspiration	– physical and chemical weathering – grain-size – mineralogical composition – bulk density – soil type – soil moisture content – carbonate content – organic material content	– relief energy – mass movements – aspect – drainage network	– land-use changes – overgrazing – water diversions
Transportation of mineral dust	– air-mass – wind speed – wind direction – convectivity and other vertical movements – precipitation (wet deposition)	– desert and soil crusts	– surface roughness – wind channels – orographic obstacles	– vegetation type and coverage

into the soil-system and increases its clay and fine-silt components even in distant areas. And at last but not least, the increased atmospheric concentration of PM_{10} and $PM_{2.5}$ particles has major effects on human health.

The global annual dust emission of mineral dust deflated from arid-semiarid areas is estimated between 1 and 3 billion of tonnes annually (Tegen, I. *et al.* 1996; Ginoux, P.M. *et al.* 2001; Zender, C.S. *et al.* 2003). Dust loadings of a given area have large annual and interannual variability controlled by several climatic and other environmental changes (*Table 1*).

The monitoring of dust storms and amount of emitted atmospheric dust can be indicative of these changes. In some periods of the Earth's history, the intensity and frequency of dust storms could have increased by several orders of magnitude compared to the present situation (Mahowald, N. *et al.* 1999, 2006; Kohfeld and Harrison, S.P. 2001). Thus, dust records of accumulated aeolian dust deposits (red clay and loess deposits; dust samples of deep-sea sediments; terrestrial material in ice-cores) are of significant importance in reconstructing past climatic and environmental processes, circulation patterns, dust source areas and emissions (Pye, K. 1987, 1995; Pécsi, M. and Schweitzer, F. 1995; Kis, É. and Schweitzer, F. 2010; Kis, É. *et al.* 2011; Újvári, G. *et al.* 2012).

Present paper is aimed at providing information on the geographical distribution and seasonality cycles of dust storms during the investigation period of 1979–2011.

Methods

Nowadays, identification and mapping of major dust source areas can be attained by various satellites, which can provide more appropriate picture on global distribution of dust storms than anecdotal observations of travellers or episodic meteorological observations. Several previous studies have confirmed that daily aerosol index (*AI*) values of NASA TOMS can be used effectively to map spatial and temporal distribution of absorbing aerosols between 70°N and 70°S latitudes (e.g. Prospero, J.M. *et al.* 2002; Washington, R. *et al.* 2003; Engelstaedter, S. *et al.* 2006; Goudie, A.S. and Middleton, N.J. 2006). These sensors (on board of different sun-synchronous NASA satellites) have the longest available global record (since 1978 November) with appropriate spatial (1×1.25 degree) and temporal (daily) resolution (Herman, J.R. *et al.* 1997; Torres, O. *et al.* 1998).

The TOMS aerosol index, as defined by NASA/GSFC Ozone Processing Team, is a measure of how much the wavelength dependence of backscattered UV radiation from an atmosphere containing aerosols (Mie scattering, Rayleigh scattering, and absorption) differs from that of a pure molecular atmosphere (pure Rayleigh scattering). The aerosol index *AI* is defined as

$$AI = 100 \log_{10}\left(\frac{I_{360}^{meas}}{I_{360}^{calc}}\right),$$

where I_{360}^{calc} is the measured 360 nm TOMS radiance, I_{360}^{calc} and is the calculated 360 nm TOMS radiance for a Rayleigh atmosphere (Herman, J.R. *et al.* 1997).

The whole database is actually a huge 3D matrix with latitude–longitude–time dimensions (*Figure 1).* The data-matrix was analysed in MathWorks' Matlab (R2007b) environment by a self-developed algorithm. With the calculations of regional daily means regional time-series were created, which data-series could be analysed by mathematical-statistical methods (identification of annual, interannual and seasonal changes). The global mean maps (e.g. monthly, seasonal and yearly means) were compiled by averaging the whole data-domains; the kriging of maps was processed in Golden Software SURFER 8. The detailed discussion of the source areas was completed with the ETOPO1 1 arc-minute global relief model (Amante, C. and Eakins, B.W. 2009) and with NASA's Blue Marble Next Generation satellite images (Stöckli, R. *et al.* 2005).

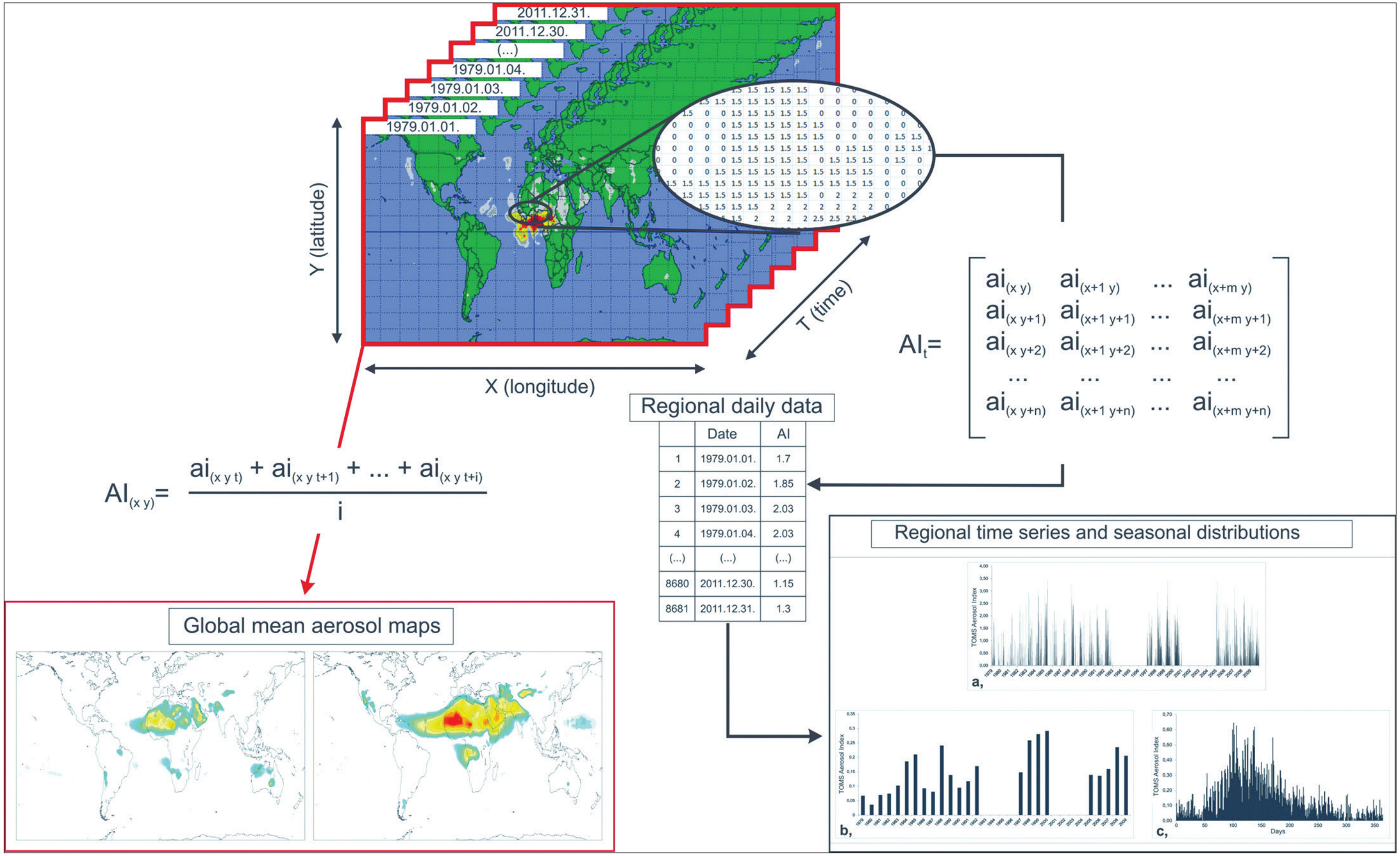

Fig. 1. Schematic illustration of the analyses

Fractional data of 1993 and 1996 (caused by satellite failure), periods with calibration problems of 2001–2004 (Kiss, P. *et al.* 2007) and 2010–2011, and four-yearly leap days (due to the matrix-operations) were excluded from the long-term mean mapping analyses (*Table 2*).

Table 2. The employed periods of TOMS AI data-matrices

Data used	Satellite	Time-series	
01/01/1979–06/05/1993	Nimbus-7	14×365 + 126	5,236 days
06/05/1993–25/07/1996	No data		
25/07/1996–31/12/2000	EarthProbe	4×365 + 160	1,620 days
01/01/2001–31/12/2004	Calibration problems		
01/01/2005–31/12/2009	Aura/OMI	5×365	1,825 days
01/01/2010–31/12/2011	Calibration problems		
01/01/1979–31/12/2011		*23×365 + 286*	*8,681 days*

Global spatial distribution of dust storms

The global mean map of the investigation period (1979–2011) shows the spatial distribution of the most important dust source areas *(Figure 2*). These are situated mainly in the desert, semi-desert regions, where dry, unconsolidated and unprotected fine-grained sediments can be easily lifted by the wind into the atmosphere. Albeit, the mechanisms responsible for silt production under warm-dry conditions have been a matter of scientific debate for many years, triggered by the absence of extent loess regions in the marginal zones of major deserts.

However, recent observations have shown that aeolian and fluvial abrasion, salt and thermal fatigue weathering may also produce large quantity of silt-sized material. Various geomorphological environments (e.g. dry and salt lakes, playas, wadis, ephemeral streams, alluvial fans) are also suitable for substantial dust generation (Assallay, A.M. *et al.* 1998; Wright, J.S. 2001; Smith, B.J. *et al.* 2002). It is important, that water (transportation by ephemeral streams or silt-storage in lacustrine environments) plays substantial role in formation of mineral dust particles, even in arid zones.

Thus, the absence of extensive loess belt around hot desert regions cannot be explained by the insufficient amount of silt-sized material, it is much more likely that loess-formation was prohibited by lack of available vegetation traps for dust. However, long-range transport of small-dust particles (<20μm) with longer atmospheric residence time could have played some role in distant loess-formation processes; e.g. Saharan dust addition to Central and South European loess deposits (Cremaschi, M. 1990; Stuut, J-B. *et al.* 2009).

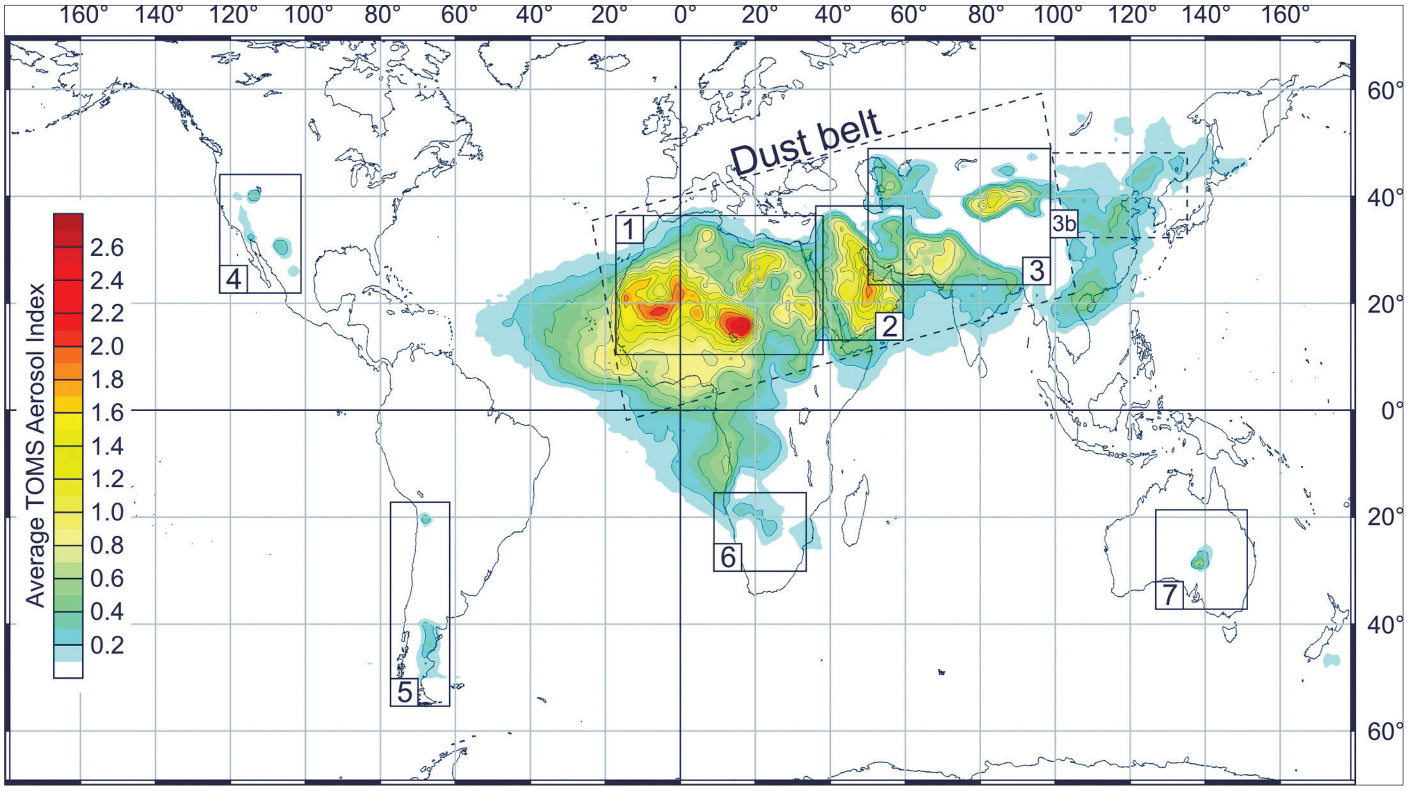

Fig. 2. Global mean map of the measured daily TOMS Aerosol Index values and locations of the discussed major dust source domains. – 1 = Saharan; 2 = Arabian; 3 = Asian; 3b = East Asian; 4 = North American; 5 = South American; 6 = South African; 7 = Australian Domain

As it is indicated by the thick loess blankets, during Pleistocene glacial periods the great ice caps produced huge amount of silty material formed by glacial grinding, but nowadays the low- and mid-latitude arid regions are regarded as the main dust source areas. Due to the spatial availability of the TOMS AI measurements (70°N–70°S), the artic regions with high aerosol emissions are not well represented at the mean maps. The high aerosol values in some equatorial regions and in East Asia are attributable to biomass burning and industrial pollution.

It is clearly visible, that major sources are creating a more or less continuous region from the west coast of North Africa, through the Middle East into the direction of Central Asia. This is the so called "Global Dust Belt" (Prospero, J.M. *et al.* 2002). The average intensity of dust emission and annual frequency of dust storms outside the dust belt are relatively low, concentrated in small distinct areas. The dominance of the source areas located in the dust belt could be noticed much more on the mean TOMS AI distribution diagrams (*Figure 3*).

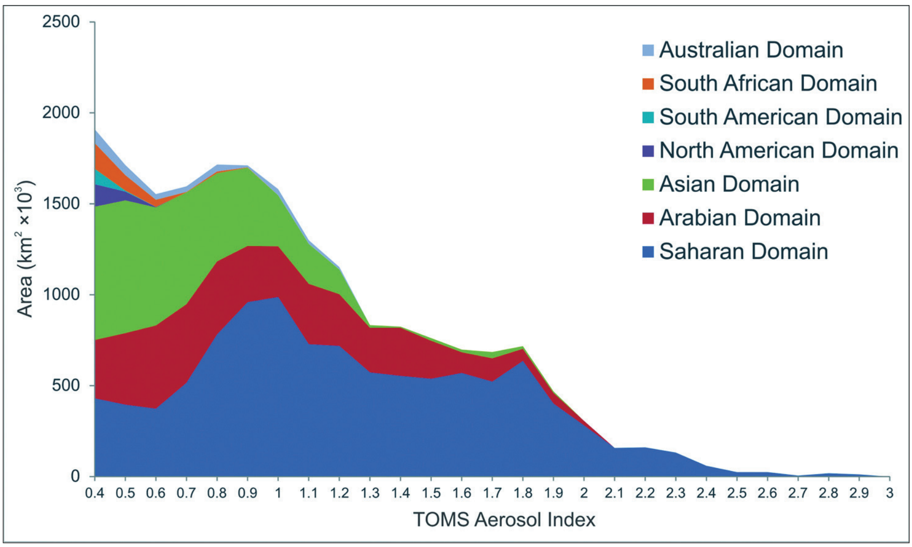

Fig. 3. Areal distribution of different TOMS AI values for the major dust source domains

Temporal distribution of dust storms

The global seasonal cycles of dust storms can be analysed by using the monthly mean aerosol maps (*Figure 4*). The source areas show large temporal variations in their dust emissions, related to various synoptic meteorological and local

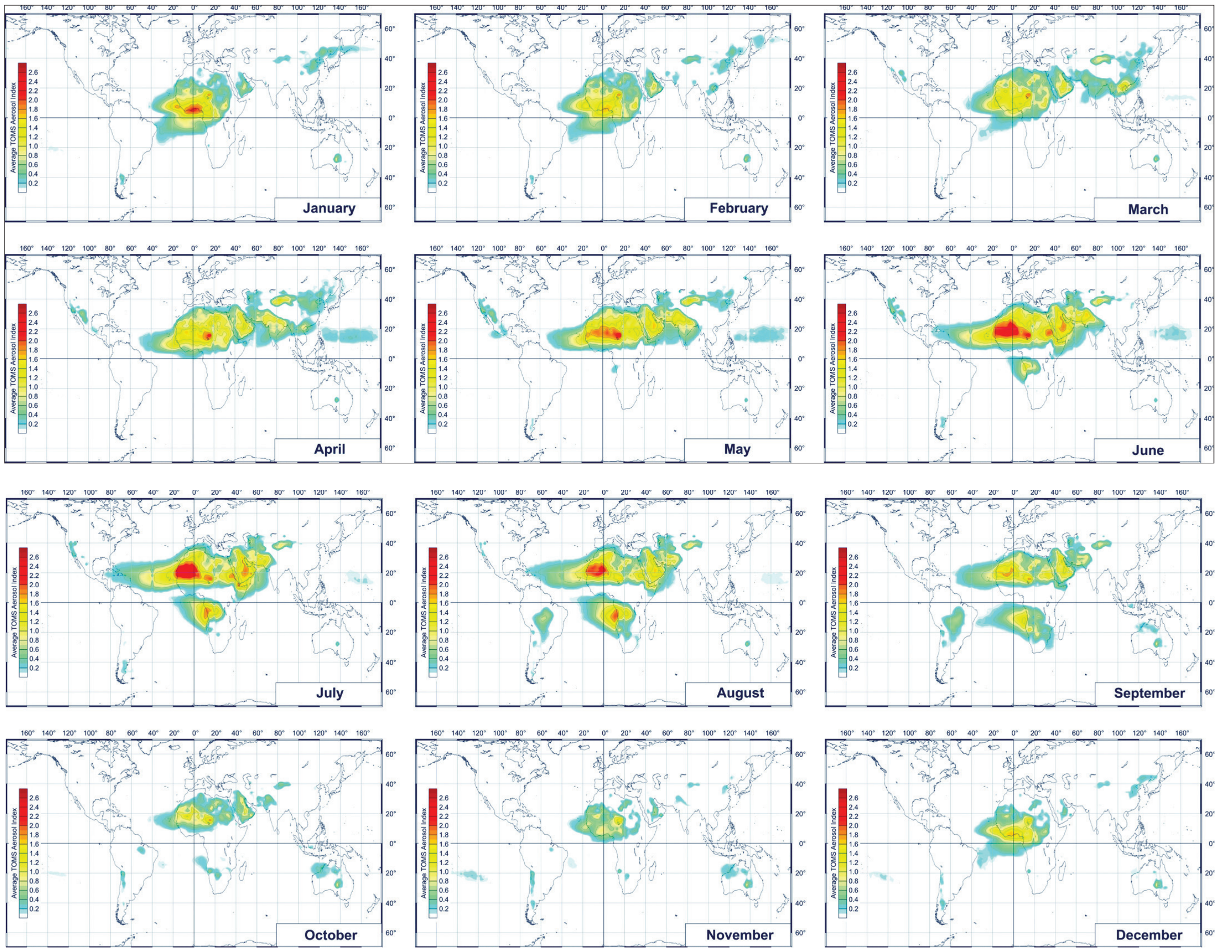

Fig. 4. Monthly mean maps of global TOMS AI values

environmental factors (e.g. distribution of precipitation, thermal convectivity and wind patterns, seasonality of cyclogenesis and other synoptic patterns, vegetation periods etc.).

In generally, it can be stated that in arid areas the seasonal maxima of dust entrainment occur typically during spring and summer, in the periods of highest wind-strengths and thermal convective activity. At some semi-arid and sub-humid, mid-latitude areas the peak of dust activity is at early spring (or late winter) before the vegetation-period, when fields are ploughed and the snow-cover has melted.

Detailed discussion of dust source areas

The appropriate spatial resolution of the satellite measurements allow us to identify distinct source areas on regional scale within the above mentioned major dust source domains and to investigate their common geomorphological and sedimentary environment. The seasonality patterns of all sources were determined by the analysis of regional time-series data. The temporal characteristics of the regions make it possible to assess typical meteorological conditions favourable for dust emission.

Saharan dust source areas

The most intensive and most important dust source areas are situated in the Sahara (and partly in the Sahelian region), responsible for 50–70% of the global mineral dust emission (Ginoux, P.M. *et al.* 2001; Miller, R.L. *et al.* 2004). Dust activity of North African sources shows large temporal variability, except for one region visible all year long, the Bodélé Depression (marked with **1.1** at *Figure 5*).

This area, considered as the largest dust source globally, is located in the large depression northeast from the Lake Chad, once part of the large Lake Mega-Chad (Washington, R. *et al.* 2006). The fine-grained mineral material of the emissions originates from the diatomite deposits of the ancient lakebed, nowadays a series of ephemeral and dry-lakes. The prevailing wind is the northeastern dry trade wind, the Harmattan strengthened by the channelling effect of the Tibesti and Ennedi Mountains.

The dominance of the single general flow direction is clearly demonstrated by the presence of large barchans and barchanoid dunes at the NE parts of the region. The ballistic impact of the saltating sand-sized grains outflowed from dunes plays important role during the entrainment of clay- and silt-sized dust material (Bagnold, R.A. 1941; Pye, K. 1987; Shao, Y. 2008). Though, dust

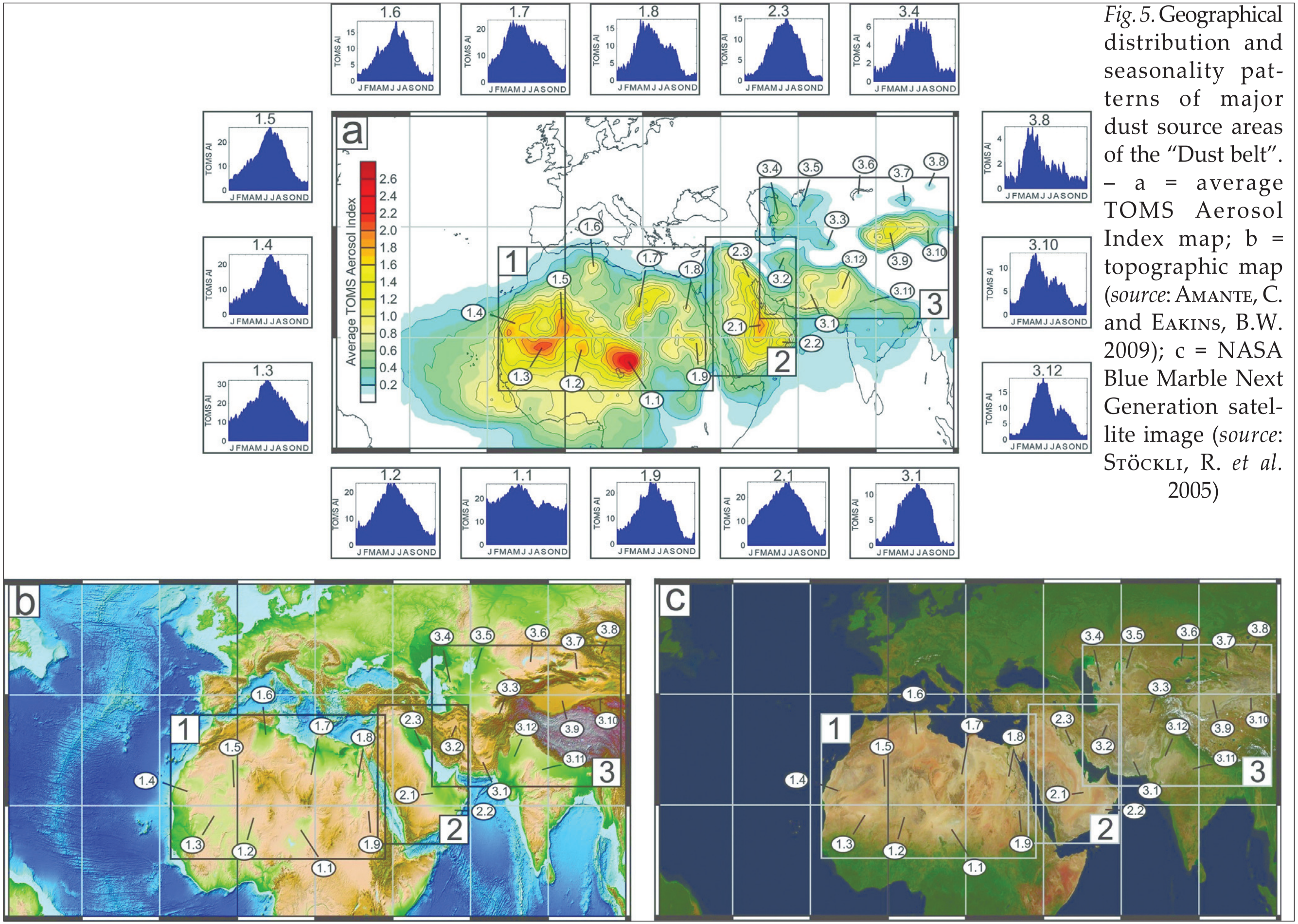

Fig. 5. Geographical distribution and seasonality patterns of major dust source areas of the "Dust belt". – a = average TOMS Aerosol Index map; b = topographic map (*source*: Amante, C. and Eakins, B.W. 2009); c = NASA Blue Marble Next Generation satellite image (*source*: Stöckli, R. *et al.* 2005)

activity persists all year long, the seasonal cycles show some seasonal variability being at the minimum in late summer. Related to the northward migration of the Intertropical Convergence Zone (ITCZ), the wind strength is reduced in July and August, when the convergence of the northerly and southerly winds is situated north from the Bodélé.

An intense isolated spot of high dust activity **(1.2)** can be found in the Azawagh (Azaouak) structural basin framed by the Adrar des Ifoghas, by the Thassili du Hoggar and by the Aïr Mountains. The Azawagh was the catchment area of an ancient northern tributary of Niger River during the Pleistocene pluvial periods (Paris, F. 1995). The dust sources of the region can be associated with alluvial deposits and the system of ephemeral streams originating from the foothills of Ahaggar (Hoggar) and the Aïr.

An extensive dust source is located in the southern part of the Taoudenni Basin NW from the large bend of Niger River and west from the Adrar des Ifoghas **(1.3)**. During the Pleistocene period the area was flooded by Lake Araouane, one of the largest pluvial lakes in Africa (Bridges, E.M. 1990). The salt and diatomite deposits of the enclosed basin can be clearly seen on satellite images. The surface of the ancient lakebed is partly covered by extensive system of barchanoid dunes formed by the prevailing NE trade winds.

The dust emission mechanism of the region is similar to the Bodélé Depression; the intensive deflation of the fine-grained particles of lacustrine deposits is enhanced by the bombardment energy of saltating sand particles. Due to human activities (intensifying irrigation and hydroelectric dam building) the braided distributaries, ephemeral streams and lakes of the Inner Niger Delta could be the next major dust source area of the region (Pearce, F. 2012).

A long narrow band of dust sources is located at the western part of the Sahara **(1.4)**, generally lying at the eastern slopes of gentle hills running parallel to the Atlantic coast. A territory of a series of seasonal streams (with frequent flash floods in the spring) and sebkhas (e.g. Sebkha Ijil) at the pedimented surface of the Adrar Souttouf and Zemmour Massif are acting as the main sources of fine-grained material in this region. Large sand seas (Erg Iguidi and Erg Chech) are situated NE from the area.

Many sources are associated with the large alluvial fans and extensive wadi-system at the W and NW slopes of the Ahaggar **(1.5)**. The Tidikelt Depression at northern part of this region, surrounded by plateaus (the Tanezrouft to the south and Plateau du Tademait to the north), by mountains (Ahaggar and Tassili-n-Ajjer to the east) and by the sand sea of Erg Chech to the west has an extensive ephemeral drainage system including several wadis from elevated regions, seasonal marshes and mud flats (Glaccum, R.A. and Prospero, J.M. 1980).

The dust activity of above discussed four regions shows similar variability throughout the year. The atmospheric dust concentration is at a maximum in late spring and summer. The dust emission of these sources is primary governed by the migration of the ITCZ and thermal convective activity of the hottest seasons.

An isolated dust hot-spot area can be found in the lowlands south of the Tell Atlas **(1.6)**. The system of salt and dry lakes acts as major source in spring and summer. Dust emission seems to be largest between and to the south of the two largest salt lakes (Chott Melrhir and Chott Jerid) lying north to the Grand Erg Oriental (Prospero, J.M. *et al.* 2002). Dust transportation from the foreland of the Atlas is mostly associated with the formation of Sharav cyclones, generated by the thermal gradient between heated land and cold Mediterranean Sea (Alpert, P. and Ziv, B. 1989; Kalderon-Asael, B. *et al.* 2009). Similar atmospheric circulation patterns are responsible for the dust emission from the dusty area expanding from the northern hillslopes of Tibesti through Cyrenaica to the Qattara Depression **(1.7)**. The main period of dust transportation from the alluvial fans, extensive wadi systems on flanks of topographic highs and ephemeral lakes in the low-lying areas is in spring with a secondary maximum in summer.

Only the low-lying areas next to the north-south trending escarpments along the Nile **(1.8)** and the region of Tokar Delta **(1.9)** can be regarded as important dust sources in the eastern part of Sahara. The alluvial deposits of the silt-laden Baraka River are the parent material of dust storms in the Tokar Delta, where gap winds channelled by the Red Sea Hills transport large quantities of mineral particles into the direction of the Red Sea (Goudie, A.S. and Middleton, N.J. 2006).

Saharan dust is often detectable over the Atlantic Ocean, Mediterranean and Red Sea, and also in the atmosphere of distant areas (*Figure 6*). Typically, four main long-range transportation routes can be distinguished: (1) westward transport of the Saharan Air Layer over the North Atlantic into the direction of North and South America (Prospero, J.M. *et al.* 1970; Swap, R. *et al.* 1992); (2) southward to Gulf of Guinea by the Harmattan (McTainsh, G. and Walker, P.H. 1982); (3) northward to Europe associated to various synoptic meteorological situations (Barkan, J. *et al.* 2005; Engelstaedter, S. *et al.* 2006; Varga, Gy. 2012); and (4) eastward to the Middle East by Sharav cyclones (Alpert, P. and Ziv, B. 1989) or by gap winds at the Tokar Delta (Goudie, A.S. and Middleton, N.J. 2006).

Arabian dust source areas

The second largest dust activity (after the Sahara) can be observed in the Arabian Domain, in the Middle East. Dust plumes cover large areas almost all year long at the Arabian Peninsula and at the Mesopotamian Plain. Three distinct source areas were distinguished in the region. The most prominent dust emission can be detected in the area of salt flats and ephemeral streams at

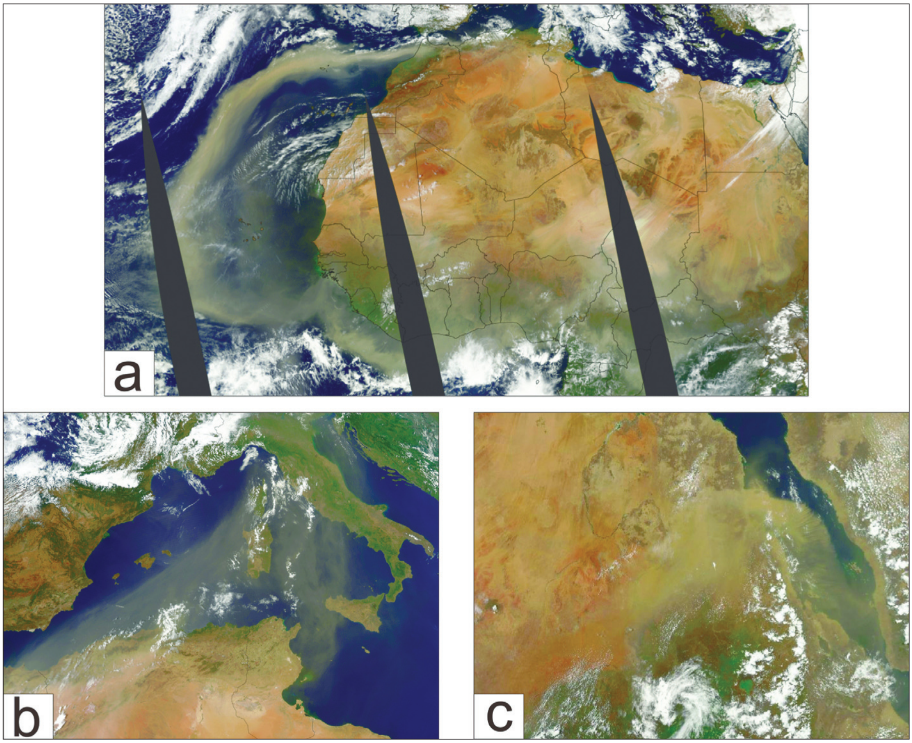

Fig. 6. NASA MODIS satellite images of long-range dust transportation from Saharan source areas. – a = North Atlantic and southward transport (June 6, 2004); b = Saharan dust over the Mediterranean Sea (July 16, 2003); c = North African dust over the Red Sea from the Tokar Delta (June 20, 2012). *Source*: NASA Earth Observatory: http://earthobservatory.nasa.gov/

the eastward facing slopes of Jebel Tuwaiq and over the coastal sabkhas at the low-lying flat terrain running parallel to the Arabian Gulf (**2.1** at *Figure 5*).

The huge sand sea of Rub' al-Khali separates these sources from the dust hot-spot area situated at the SE part of the Arabian Peninsula in Oman **(2.2)**. The isolated circle shaped area with high TOMS AI values is located direct above an inland sabkha system in the low-lying areas fed by wadis from the southern coastal mountainous region of Jebel Dhofar. The dominant dust sources of the Arabian Peninsula are situated in depressions or at the flanks of topographic highs bordered by large sand seas. The main period of dust storms is spring and summer.

Dust activity of the Tigris-Euphrates Basin **(2.3)** can be connected to a different kind of geomorphological environment. At northern territory of the Persian Gulf, floodplain deposits and extensive marshlands of the two large rivers provide the main source of deflated fine-grained mineral material. The seasonal cycle of dust emission observed by TOMS AI shows same variability; the maximum dust transport occurs in spring and summer and it is at a minimum in winter.

There are several named dust-bearing winds in the Arabian Domain (e.g. belat, simoom, shargi), but the most dusty episodes are caused by the northwesterly shamal winds (Goudie, A.S. and Middleton, N.J. 2006). The high wind-speeds are associated with a steep pressure gradient between the intense summer heat low over Pakistan and Afghanistan and the semi-permanent anticyclonal centre over NW Saudi Arabia (Pye, K. 1987).

Asian dust source areas

Arid-semiarid endorheic basins among high mountain belts, extensive flat terrains, deserts and hyper-continental climate provide suitable conditions for dust emission at several regions of the Asian Domain. Anthropogenic factors also play important role at some places, where the unreasonable constructions of irrigation channels and other agricultural activities have enhanced the dust activity by several orders of magnitude during recent decades.

The most prominent dust sources of SW Asia are associated to shallow saline and dry lakes situated in closed basins, depressions between high mountainous belts and are fed by fine-grained material from these neighbouring elevated regions. According to TOMS AI maps, a cluster of major dust sources are located at the southern flanks of the Makran Coastal Range and in the Sistan (Seistan) Basin (**3.1** at *Figure 5*).

The geomorphological environment of the intermountain basins can be characterized by alluvial fans, wadis, swamps, marshes and a series of shallow lakes, known as hamouns in this region (Middleton, N.J. 1986). The largest ephemeral lakes are Hamoun-e Puzak, Hamoun-e Sabari and Hamoun-e Helmand; these intensive dust sources are the remnants of a once more humid climatic regime at the Hamoun wetlands (Partow, H. ed. 2006). Dust plumes cover large areas also at the NW part of Iranian Plateau, where huge salt flats (kavirs) are covering the wide arid basins of Dasht-e Kavir and Dasth-e Lut deserts **(3.2)**. The small intermountain valley of Fergana **(3.3)** has also a significant dust activity in the region.

Strong katabatic winds funnelled by gaps in the high mountains and thunderstorm downdrafts are causing dust storms especially during the summer months (in July and August), however the dust activity is fairly high from April to October. Dust outbreaks originated from SW Asian sources can often be observed over the Arabian Sea (*Figure 7*).

Several distinct dust sources can be identified at the Turan Plain and at the northern foothills of Central Asian high mountains mostly associated with shallow or dried lakes, ancient lakebeds and alluvial fans (Goudie, A.S. and Wells, G.L. 1995; Prospero, J.M. *et al.* 2002). TOMS AI maps show intensive dust

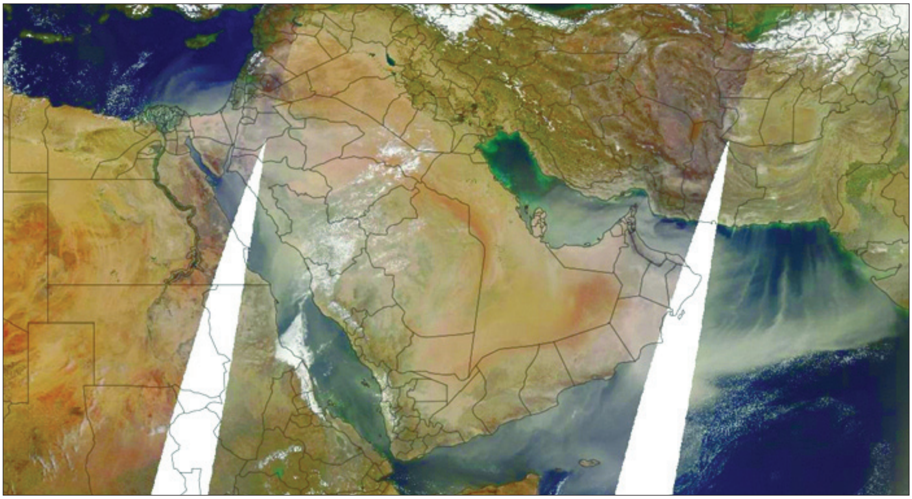

Fig. 7. Massive dust outbreak over the Arabian Sea originated from SW Asian source regions (March 20, 2012). *Source*: NASA LANCE-MODIS Web Mapping Service: http://lance-modis.eosdis.nasa.gov/wms)

emission at the eastern shores of Caspian Sea, direct over the Kara-Bogaz Gol **(3.4)**. The ancient gulf of the lake was dried out as a consequence of construction of an embankment (Gill, T.E. 1996). Another example of anthropogenic environmental disaster areas and another dust hotspot is located in the region, the territory of Aral Sea **(3.5)**. TOMS measurements clearly show that the dried-out deltas of Amu Darya and Syr Darya rivers and the exposed lakebed of shrinking Aral Sea are extensive sources of windblown fine-grained material.

An isolated dust source area is located in the complex drainage basin of Lake Balkhas **(3.6)**. The thick alluvial deposits of the seven feeding rivers and the arid climate of Balkhas-Alakol Basin are providing suitable conditions to effective dust emission. The cold fronts of eastward moving low-pressure atmospheric systems are generating strong winds in the spring, which is the main period of dust activity in the region. Similar synoptic meteorological conditions are responsible for dust storms in the Junggar Basin **(3.7)** and in the Uvs Lake Basin **(3.8)**. These endorheic basins are surrounded by high mountain belts fed by fine-grained material from alluvial fans and ephemeral streams, similarly to other "High Asian" sources.

The largest and most persistent dust source region in Asia is located in the Tarim Basin **(3.9)**. The huge sand sea of Taklimakan desert is bounded by the Himalayan Plateau, Hindu Kush and Tien Shan. At marginal areas of the sandy desert areas extensive ephemeral drainage systems, seasonal lakes and alluvial fans can be identified. The extensive desert area has been a significant dust source region since the Late Miocene as it is demonstrated by the thick aeolian dust deposits at its flanks and at the Chinese Loess Plateau (Liu, T.S. *et al.* 1985; Zheng, H. *et al.* 2003). TOMS AI measurements show intensive dust emission also at the eastern flanks of the large desert area. These high aerosol values can be connected to the salt flat of Lop Nor and the intermountain Quaidam Basin **(3.10)**.

The dust plumes can be observed all year long over the area, but the highest concentrations of atmospheric dust is most clearly visible on the TOMS AI maps during early spring with a secondary maximum in summer months. Dust material deflated from the Tarim Basin commonly reaches the North Pacific Ocean (Duce, R.A. *et al.* 1980), North America (Jaffe, D.A. *et al.* 1999) or in particular cases, Europe (Grousset, F.E. *et al.* 2003).

Different kinds of dust source areas are lying at the northern part of the Indian Subcontinent. The large alluvial plains of Indus and Ganges **(3.11)** are receiving huge amount of fine-grained material from the bordering Himalayas. The extensive desert area of Thar **(3.12)**, next to the Indus floodplain also serves as a major source area. Dust activity peaks in spring and late summer, with a considerable drop around the arrival of monsoonal rains.

The thickness of Plio-Pleistocene aeolian dust deposits (red clay and loess) exceeds the 300 metres at some places of Chinese Loess Plateau, presenting a once dustier epoch of the region (Liu, T.S. *et al.* 1985).

Nowadays, the area has been regarded also as a territory with high dust loads. However it is difficult to map by TOMS the distribution atmospheric dust and exactly locate the present-day source areas, because of the presence of large amounts of industrial pollutants. According to meteorological data (Middleton, N.J. 1986) and field observations (Derbyshire, E. *et al.* 1998) Gobi, Badain Jaran, Tengger, Ulan Buh deserts and the Hexi corridor are the main sources in Eastern Asia. Due to the intense agricultural activity, the damaged soils of the Loess Plateau are also intense dust sources (Goudie, A.S. and Middleton, N.J. 2006).

North American dust source areas

Dust activity in the region is visible on TOMS aerosol maps from March to August in the SW part of the United States and in northern Mexico (*Figure 8*). Several isolated source regions are situated in the Great Basin bordered by high mountain ranges of Rocky Mountains, Sierra Nevada and Cascades running parallel to the Pacific coast of North America. The internal drainage system of the contiguous intermountain highland basins can be characterized by distinct salt flats, playas, shallow lakes and deep alluvial deposits of fans (Muhs, D.R. in press).

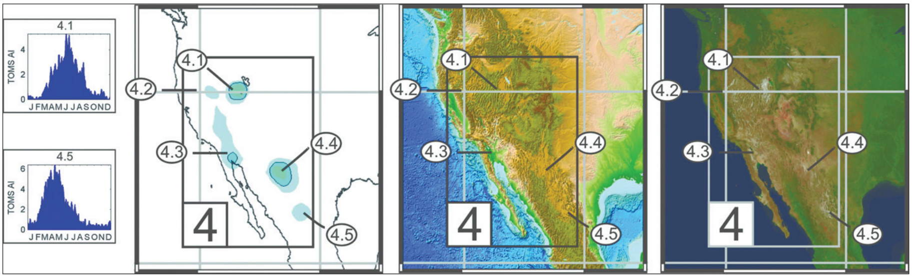

Fig. 8. Geographical distribution and seasonality patterns of major dust source areas in North America

One of the most intense sources is located direct to the SW of Great Salt Lake (**4.1** at *Figure 8*). The lake and the surrounding salt flats of Great Salt Lake Desert, Tule Dry Lake and Sevier Dry Lake are remnant of prehistoric pluvial Lake Bonneville. Similar, but smaller dust source area is located in the Smoke Creek and Black Rock Deserts north to the Pyramid Lake, remnant of Pleistocene pluvial Lake Lahontan **(4.2.)**. Deflation from these ancient, barren lake beds are associated with the passage of strengthening low pressure systems and the related prefrontal winds (Hahnenberg, M. and Nicoll, K. 2012).

Dust emission is also intense from the playa system of Salton Sink in the Coachella and Imperial valleys of southeastern California **(4.3)**. The low-lying pull-apart basin was covered by prehistoric Lake Cahuilla in the Late Pleistocene and Early Holocene (Babcock, E.A. 1974). The steep-pressure gradient between the anticyclonal Pacific High centre and the approaching low-pressure cells creates suitable conditions for dust emission in spring and early summer (Pye, K. 1987).

Two relevant source areas can be observed at the Mexican Altiplano (or Central Mexican Plateau). The plateau area is bounded by the Sierra Madre Occidental and Sierra Madre Oriental; extensive playa systems and alluvial fans are covering its diverse surface. The northern spot of high dust activity is associated with the arid basins and depressions of the Chihuahuan Desert **(4.4)**, while the southern, less active source area is situated in the endorheic basin of Bolsón de Mapimí **(4.5)**. Dust plumes cover large areas in the region during early spring, and as the season progresses dust activity expands to the northwest.

Dust storms at high latitude areas of North America in Alaska (from glacial outwash plains) and in Canadian Prairies, and also at the Great Plains are common; however TOMS measurements cannot represent well these sources, because of aerosol emission is restricted to the lower levels of the troposphere (Herman, J.R. *et al.* 1997).

Three different clusters of dust source areas can be identified by the TOMS AI maps in South America (*Figure 9*). Many isolated sources are associated with the salt flats (salars) located in the internal drainage system of high plateau region of Altiplano flanked by the Oriental and Occidental Cordilleras of the Andes (**5.1** at *Figure 9*). Most remarkable source area is the Salar de Uyuni, the largest salt flat of the Earth. The deep halite deposits of the flats have been accumulated during the Pleistocene pluvials, when large lakes covered the Altiplano's depressions (from north to south: Titicaca, Poópo, Coipasa, and Uyuni) (Placzek, C.J. *et al.* 2011). Nowadays, these ancient lacustrine deposits serve as major source of present-day dust storms in the region, where dusty activity peaks in September–November (Prospero, J.M. *et al.* 2002).

The long narrow band of sources at the eastern slopes of Southern Andes **(5.2)** is active in the second part of the year. Katabatic winds flow out fine-grained particles from alluvial deposits of piedmont area and from extensive series of salt flats, marshes and salinas.

Plio-Pleistocene loess and loess-like deposits cover huge areas in the Patagonia, representing a predominant role of aeolian sedimentation in the region. Recent aerosol maps also show intensive summer and winter dust activity at the Pampas **(5.3)**.

Westerly winds flowing down from the high mountain regions of the Andes transport huge amount of deflated fine-grained particles from glacial,

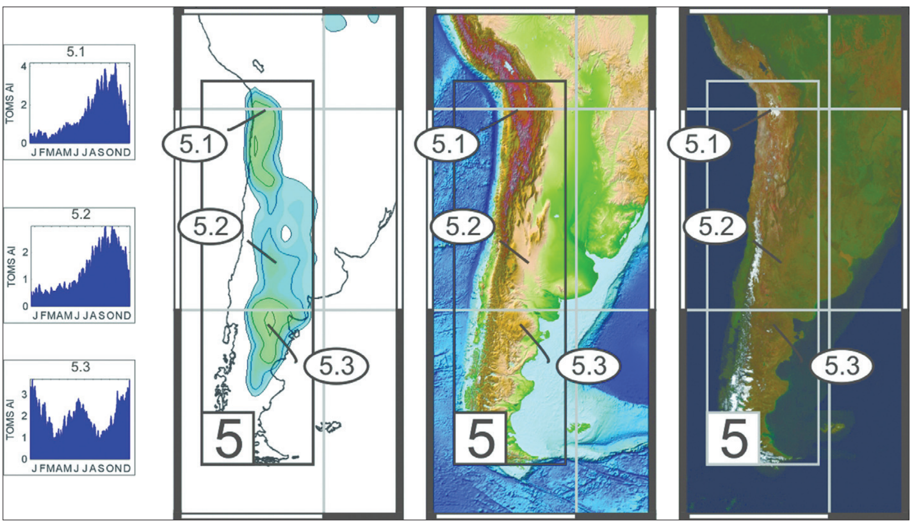

Fig. 9. Geographical distribution and seasonality patterns of major dust source areas in South America

fluvioglacial and volcanic deposits of arid areas lying in rain shadow at easterly slopes of the mountain belt. By its long range transport, Patagonian dust is the main constituent of aeolian deposits trapped in West Antarctic glaciers (Sugden, D.E. *et al.* 2009).

South African dust source areas

Despite to the fact that, there is seasonally huge amount of aerosol particles in South African atmosphere, this is primary related to biomass burnings, and dust emission is restricted to two, relatively small but fairly effective source areas (*Figure 10*). These two dust hot-spots are located over the endorheic basins of Etosha Pan (**6.1** at *Figure 10*) and Makgadikgadi Depression **(6.2)**.

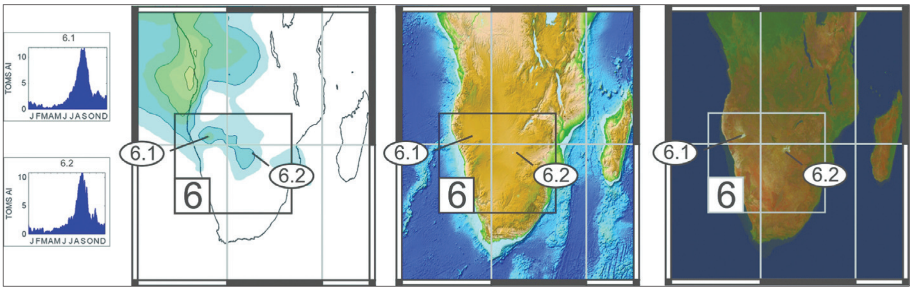

Fig. 10. Geographical distribution and seasonality patterns of major dust source areas in South Africa

Surface of the Etosha Pan is covered by deposits of ephemeral lakes and swamps, and by sediments of former inner delta of Cunene River, which fed the Paleolake Etosha during the pluvial phases of Pleistocene (Goudie, A.S. 1996). Similarly to the other South African source area, Makgadikgadi Depression was also covered by a large pluvial lake in the past. The several salt flats and pans (seasonally flooded by the Boteti River) are the remnants of the Pleistocene Lake Makgadikgadi. Dust activity peaks in August and September, just before the arrival of moister season.

Australian dust source areas

Dust emission of Australia can be connected to one dominant and three weaker source areas (*Figure 11*). Most of atmospheric dust is originated from the mostly dry, large playa system of Lake Eyre basin, a persistent and significant southern hemisphere dust source (**7.1** at *Figure 11*). The fine-grained mineral

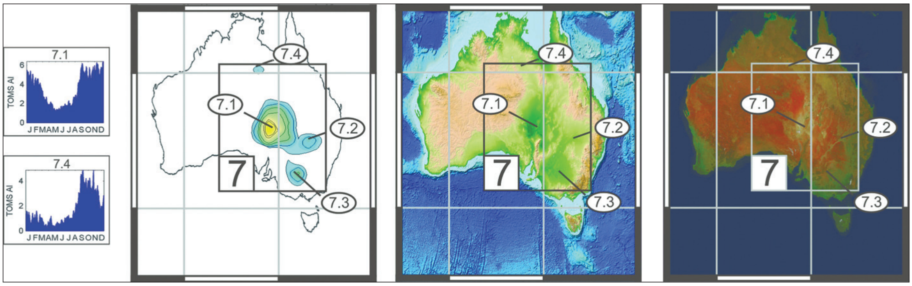

Fig. 11. Geographical distribution and seasonality patterns of major dust source areas in Australia

material of the internal drainage system of playas fed by ephemeral rivers, streams and creeks, floodplain and former aeolian dust deposits are deflated out during austral spring and summer, from September to March.

Other two sources are located in the Murray-Darling Basin. The northern spot of dust activity **(7.2)** can be connected to floodplain deposits of River Darling and its ephemeral tributaries, and to salt swamps (e.g. Caryapundy Swamp). The southern source area is the low-lying region of River Murray **(7.3)**, characterized by floodplain deposits, intermittent salt lakes and swamps. Weak and occasional dust activity can be observed by TOMS over the playas at the SW side of Barkly Tableland **(7.4)**.

Major dust-outbreaks in Australia are related to pre-frontal northerly and postfrontal southerly winds of eastward moving low-pressure systems (Strong, C.L. *et al.* 2011). These two wind-systems determine the offshore dust transportation from Australia into the directions of Southern Pacific and Indian Oceans. The presence of varied aeolian deposits (parna, loess and loess-like deposits, wind-blown sand dunes) shows us, that the region has a long aeolian geomorphological history (Hesse, P.P. and McTainsh, G.H. 2003; Fitzsimmons, K.E. *et al.* 2009).

Summary

Analyses of NASA's TOMS aerosol measurements have demonstrated that the spatial distribution of dust storms are associated to specific geomorphological environments, while emissions show large seasonal variability related to regional meteorological conditions. Areas with high TOMS AI values are lying in arid-semiarid regions, mostly in geomorphological depressions or at flanks of high mountains. The fine-grained dust material of the sources is the product of former fluvial or lacustrine sedimentary environments.

Most of the major sources are situated on remnants of large Pleistocene pluvial lakes, which are nowadays almost totally dried up. The hardened surface of ancient lakebeds can disrupt by bombardment of larger particles, and so the barren deep alluvial deposits are very susceptible to wind erosion. Playas, sabkhas, pans and other ephemeral salt lakes and flats bordered by large sand seas are the largest and most persistent dust source areas of our planet.

REFERENCES

Alpert, P. and Ziv, B. 1989. The Sharav Cyclone: Observations and some theoretical considerations. *Journal of Geophysical Research* 94. 18495–18514.

Amante, C. and Eakins, B.W. 2009. ETOPO1 1 Arc-Minute Global Relief Model: Procedures, Data Sources and Analysis. *NOAA Technical Memorandum NESDIS NGDC* 24. 19 p.

Arimoto, R. 2001. Eolian dust and climate: relationships to sources, tropospheric chemistry, transport and deposition. *Earth-Science Reviews* 54. 29–42.

Assallay, A.M., Rogers, C.D.F., Smalley, I.J. and Jefferson, I.F. 1998. Silt: 2–62 μm, 9–4 Φ. *Earth-Science Reviews* 45. (1–2): 61–88.

Babcock, E.A. 1974. Geology of the northeast margin of the Salton trough, Salton Sea, California. *Geological Society of America Bulletin* 85. 321–322.

Bagnold, R.A. 1941. *The physics of blown sand and desert dunes.* London, Methuen, 265 p.

Barkan, J., Alpert, P., Kutiel, H. and Kishcha, P. 2005. Synoptics of dust transportation days from Africa toward Italy and central Europe. *Journal of Geophysical Research. Atmospheres* 110. D07208. 14 p.

Bridges, E.M. 1990. *World Geomorphology*. Cambridge, Cambridge University Press, 272 p.

Cremaschi, M. 1990. The loess in northern and central Italy; a loess basin between the Alps and the Mediterranean regions. In *The loess in northern and central Italy; a loess basin between the Alps and the Mediterranean region.* Ed. Cremaschi. Milano, Dipartimento de Scienze della Terra dell'Universita degli Studi Milano. Sezione di Geologia e Paleontologia, Nuova Serie 602. 15–19.

Derbyshire, E., Meng, X. and Kemp, R.A. 1998. Provenance, transport, and characteristics of modern aeolian dust in western Gansu Province, China, and interpretation of the Quaternary loess record. *Journal of Arid Environments* 39. (3): 497–516.

Duce, R.A., Unni, C.K., Ray, B.J., Prospero, J.M. and Merrill, J.T. 1980. Long-range atmospheric transport of soil dust from Asia to the tropical North Pacific: temporal variability. *Science* 209. (4464): 1522–1524.

Engelstaedter, S., Tegen, I. and Washington, R. 2006. North African dust emissions and transport. *Earth-Science Reviews* 79. (1–2): 73–100.

Fitzsimmons, K.E., Magee, J.W. and Amos, K.J. 2009. Characterisation of aeolian sediments from the Strzelecki and Tirari Deserts, Australia: Implications for reconstructing palaeoenvironmental conditions. *Sedimentary Geology* 218. (1–4): 61–73.

Gill, T.E. 1996. Eolian sediments generated by anthropogenic disturbance of playas: human impacts on the geomorphic system and geomorphic impacts on the human system. *Geomorphology* 17. (1–3): 207–228.

Ginoux, P.M., Chin, I., Tegen, I., Prospero, J., Holben, M., Dubovik, O. and Lin, S.J. 2001. Global simulation of dust in the troposhere: model description and assessment. *Journal of Geophysical Research* 106. 20255–20273.

Glaccum, R.A. and Prospero, J.M. 1980. Saharan aerosols over the tropical North Atlantic: mineralogy. *Marine Geology* 37: 295–321.
Goudie, A.S. 1996. Climate, past and present. In *The Physical Geography of Africa.* Eds.: Adams, W.M., Goudie, A.S. and Orme, A.R. New York, Oxford University Press, 452 p.
Goudie, A.S. and Middleton, N.J. 2006. *Desert Dust in the Global System*. Springer, 287 p.
Goudie, A.S. and Wells, G.L. 1995. The nature, distribution and formation of pans in arid zones. *Earth-Science Reviews* 38. (1): 1–69.
Grousset, F.E., Ginoux, P., Bory, A. and Biscaye, P.E. 2003. Case study of a Chinese dust plume reaching the French Alps. *Geophysical Research Letters* 30. (6): 1277–1280.
Hahnenberger, M. and Nicoll, K. 2012. Meteorological characteristics of dust storm events in the eastern Great Basin of Utah, U.S.A. *Atmospheric Environment* 60. 601–612.
Harrison, S.P., Kohfeld, K.E., Roelandt, C. and Claquin, T. 2001. The role of dust in climate changes today, at the last glacial maximum and in the future. *Earth-Science Reviews* 54. (1–3): 43–80.
Herman, J.R., Bhartia, P.K., Torres, O., Hsu, C., Seftor, C. and Celarier, E. 1997. Global distribution of UV-absorbing aerosols from Nimbus 7 TOMS data. *Journal of Geophysical Research Atmospheres* 102. (D14): 16911–16922.
Hesse, P.P. and McTainsh, G.H. 2003. Australian dust deposits: modern processes and the Quaternary record. *Quaternary Science Reviews* 22. (18–19): 2007–2035.
Jaffe, D.A., Anderson, T., Covert, D., Kotchenruther, R., Trost, B., Danielson, J., Simpson, W., Berntsen, T., Karlsdottir, S., Blake, D., Harris, J., Carmichael, G. and Itsushi, U. 1999. Transport of Asian air pollution to North America. *Geophysical Research Letters* 26. (6): 711–714.
Kalderon-Asael, B., Erel, Y., Sandler, A. and Dayan, U. 2009. Mineralogical and chemical characterization of suspended atmospheric particles over the east Mediterranean based on synoptic-scale circulation patterns. *Atmospheric Environment* 43. (25): 3963–3970.
Kis, É. and Schweitzer, F. 2010. Dust accumulation and loess formation under the oceanic semiarid climate of Tenerife, Canary Islands. *Hungarian Geographical Bulletin* 59. (2): 207–230.
Kis, É., Schweitzer, F., Futó, I., Vodila, G., Balogh, J. and Di Gléria, M. 2011. Special paleogeographic characteristics and changes in $\delta^{18}O$ values in Upper Pleistocene deposits of the Moravian Plateau. *Hungarian Geographical Bulletin* 60. (3): 247–259.
Kiss, P., Jánosi, I. and Torres, O. 2007. Early calibration problems detected in TOMS Earth-Probe aerosol signal. *Geophysical Research Letters* 34. (7): L07803. 5 p.
Kohfeld, K.E. and Harrison, S.P. 2001. DIRTMAP: the geological record of dust. *Earth-Science Reviews* 54. (1–3): 81–114.
Kohfeld, K.E. and Tegen, I. 2007. Record of Mineral Aerosols and Their Role in the Earth System. *Treatise on Geochemistry* 4. (13): 1–26.
Liu, T.S. *et al.* 1985. *Loess and the Environment*. Beijing, China Ocean Press, 249 p.
Maher, B.A., Prospero, J.M., Mackie, D., Gaiero, D., Hesse, P.P. and Balkanski, Y. 2010. Global connenctions between aeolian dust, climate and ocean biogeochemistry at the present day and at the last glacial maximum. *Earth-Science Reviews* 99. 61–97.
Mahowald, N., Kohfeld, K., Hansson, M., Balkanski, Y., Harrison, S.P., Prentice, I.C., Schulz, M. and Rodhe, H. 1999: Dust sources and deposition during the last glacial maximum and current climate: a comparison of model results with paleodata from ice cores and marine sediments. *Journal of Geophysical Research* 104. 15895–15916.
Mahowald, N.M., Muhs, D.R., Levis, S., Rasch, P.J., Yoshioka, M., Zender, C.S. and Luo, C. 2006. Change in atmospheric mineral aerosols in response to climate: Last gla-

cial period, preindustrial, modern, and doubled carbon dioxide climates. *Journal of Geophysical Research* 111. D10202. 22 p.

McTainsh, G.H. and Walker, P.H. 1982. Nature and distribution of Harmattan dust. *Zeitschrift für Geomorphologie* 26 (4): 417–435.

Middleton, N.J. 1986. *The geography of dust storms*. Oxford, University of Oxford, Doctoral thesis, 591 p.

Miller, R.L., Tegen I. and Perlwitz, J. 2004. Surface radiative forcing by soil dust aerosols and the hydrologic cycle. *Journal of Geophysical Research. Atmospheres* 109. D04203, 24 p.

Muhs, D.R. The geologic records of dust in the Quaternary. *Aeolian Research* (in press)

Paris, F. 1995. Le Bassin de l'Azawagh: pleuplements et civilisations, de néolithique á l'arrivée de l'islam. In *Milieux, sociétés et archéologues.* Ed.: Marliac, A. Karthala, 227–260.

Partow, H. (ed.) 2006. *History of Environmental Change in the Sistan Basin – Based on Satellite Image Analysis: 1979–2005.* Geneva, UNEP Post-Conflict Branch, 60 p.

Pearce, F. 2012. Inner Niger delta set to mimic the Aral Sea disaster. *New Scientist* 213. (2857): 9.

Pécsi, M. and Schweitzer, F. 1995. The lithostratigraphical, chronostratigrphical sequence of Hungarian loess profiles and their geomorphological position. In *Concept of loess, loess-paleosol stratigraphy.* Loess InForm 3. Eds.: Pécsi, M. and Schweitzer, F. Budapest, Geographical Research Institute of HAS, 31–61.

Placzek, C.J., Quade, J. and Patchett, P.J. 2011. Isotopic tracers of paleohydrologic change in large lakes of the Bolivian Altiplano. *Quaternary Research* 75. (1): 231–244.

Pósfai, M. and Buseck, P.R. 2010. Nature and climate effects of individual tropospheric aerosol particles. *Annual Review of Earth and Planetary Sciences* 38. 17–43.

Prospero, J.M., Bonatti, E., Schubert, C. and Carlson, T.B. 1970. Dust in the Caribbean atmosphere traced to an African dust storm. *Earth and Planetary Science Letters* 9. (3): 287–293.

Prospero, J.M., Ginoux, P.M., Torres, O., Nicholson, S.E. and Gill, T.E. 2002. Environmental characterization of global sources of atmospheric soil dust identified with the Nimbus-7 Total Ozone Mapping Spectrometer (TOMS) absorbing aerosol product. *Reviews of Geophysics* 40. 31 p.

Pye, K. 1987. *Aeolian Dust and Dust Deposits.* London, Academic Press, 334 p.

Pye, K. 1995. The nature, origin and accumulation of loess. *Quaternary Science Reviews* 14. (7–8): 653–667.

Ridgwell, A.J. 2002: Dust in the Earth system: the biogeochemical linking of land, air and sea. *Philosophical Transactions of the Royal Society A.* 360. 2905–2924.

Roda, F., Bellot, J., Avila, A., Escarre, A., Pinol, J. and Terradas, J. 1993. Saharan dust and the atmospheric inputs of elements and alkalinity to Mediterranean ecosystems. *Water, Air, and Soil Pollution* 66. 277–288.

Rogora, M., Mosello, R. and Marchetto, A. 2004. Long-term trends in the chemistry of atmospheric deposition in northwestern Italy: the role of increasing Saharan dust deposition. *Tellus B* 56. (5): 426–434.

Rosenfeld, D., Rudich, Y. and Lahav, R. 2001. Desert dust suppressing precipitation: a possible desertification feedback loop. *Proceedings of the National Academy of Sciences USA* 98. 5975–5980.

Sassen, K., DeMott, P.J., Prospero, J.M. and Poellot, M.R. 2003. Saharan dust storms and indirect aerosol effects on clouds: CRYSTALFACE results. *Geophysical Research Letters* 30. (12): 1633, 4 p.

Shao, Y. 2008. *Physics and Modelling of Wind Erosion.* (2nd revised and expanded edition). Springer, 452 p.

Shao, Y., Wyrwoll, K.H., Chappell, A., Huang, J., Lin, Z., McTainsh, G.H., Mikami, M.,Tanaka, T.Y., Wangh, X. and Yoon, S. 2011. Dust cycle: An emerging core theme in Earth system science. *Aeolian Research* 2. 181–204.

Smith, B.J., Wright, J.S. and Whalley, W.B. 2002. Sources of non-glacial, loess-size quartz silt and the origins of „desert loess". *Earth-Science Reviews* 59. (1–4): 1–26.

Stöckli, R., Vermote, E., Saleous, N., Simmon, R. and Herring, D. 2005. *The Blue Marble Next Generation - A true color earth dataset including seasonal dynamics from MODIS*. Published by the NASA Earth Observatory

Strong, C.L., Parsons, K., McTainsh, G.H. and Sheehan, A. 2011. Dust transporting wind systems in the lower Lake Eyre Basin, Australia: A preliminary study. *Aeolian Research* 2. (4): 205–214.

Stuut, J-B.W., Smalley, I. and O'Hara-Dhand, K. 2009. Aeolian dust in Europe: African sources and European deposits. *Quaternary International* 198. (1–2): 234–245.

Sugden, D.E., McCulloch, R.D., Bory, A.J.M. and Hein, A.S. 2009. Influence of Pata-gonian glaciers on Antarctic dust deposition during the last glacial period. *Nature Geoscience* 2. 281–285.

Swap, R., Garstang, M., Greco, S., Talbot, R. and Kallberg, P. 1992. Saharan dust in the Amazon Basin. *Tellus B* 44. (2): 133–149.

Tegen, I., Lacis, A.A. and Fung, I. 1996. The influence of mineral aerosols from disturbed soils on climate forcing. *Nature* 380. 419–422.

Torres, O., Bhartia, P.K., Herman, J.R., Ahmad, Z. and Gleason, J. 1998. Derivation of aerosol properties from a satellite measurements of backscattered ultraviolet radiation: Theoretical basis. *Journal of Geophysical Research Atmospheres* 103. (D14): 17099–17110.

Újvári, G., Varga, A., Ramos, F.C., Kovács, J., Németh, T. and Stevens, T. 2012. Evaluating the use of clay mineralogy, Sr–Nd isotopes and zircon U–Pb ages in tracking dust provenance: An example from loess of the Carpathian Basin. *Chemical Geology* 304–305. 83–96.

Varga, Gy. 2012. Szaharai eredetű por a Kárpát-medence légkörében (Saharan dust in the atmosphere of the Carpathian Basin.) *Földrajzi Közlemények* 136. (2): 106–123.

Washington, R.,Todd, M., Middleton, N.J. and Goudie, A.S. 2003. Dust-storm source areas determined by the Total Ozone Monitoring Spectrometer and surface observations. *Annals of the Association of American Geographers* 93. (2): 297–313.

Wright, J. 2001. „Desert" loess versus „glacial" loess: quartz silt formation, source areas and sediment pathways in the formation of loess deposits. *Geomorphology* 36. (3–4): 231–256.

Zender, C.S., Bian, H.S. and Newman, D. 2003. Mineral Dust Entrainment and Deposition (DEAD) model: Description and 1990s dust climatology. *Journal of Geophysical Research Atmospheres* 108. 4416. 19 p.

Zheng, H., Powell, C.McA., Butcher, K. and Cao, J. 2003. Late Neogene loess deposition in southern Tarim Basin: tectonic and palaeoenvironmental implications. *Tectonophysics* 375. (1–4): 49–59.